

The $0\nu\beta\beta$ -decay nuclear matrix elements with self-consistent short-range correlations

Fedor Šimkovic,^{1,2,3} Amand Faessler,¹ Herbert Mütter,¹ Vadim Rodin,¹ and Markus Stauf⁴

¹*Institute für Theoretische Physik der Universität Tübingen, 72076 Tübingen, Germany*

²*Bogoliubov Laboratory of Theoretical Physics, JINR, 141 980 Dubna, Moscow region, Russia*

³*Department of Nuclear Physics, Comenius University, Mlynská dolina F1, 842 15 Bratislava, Slovakia*

⁴*School of Physics and Astronomy, University of Manchester Manchester, M13 9PL, England*

(Dated: November 4, 2018)

A self-consistent calculation of nuclear matrix elements of the neutrinoless double beta decays ($0\nu\beta\beta$) of ^{76}Ge , ^{82}Se , ^{96}Zr , ^{100}Mo , ^{116}Cd , ^{128}Te , ^{130}Te and ^{130}Xe is presented in the framework of the renormalized quasiparticle random phase approximation (RQRPA) and the standard QRPA. The pairing and residual interactions as well as the two-nucleon short-range correlations are for the first time derived from the same modern realistic nucleon-nucleon potentials, namely from charge-dependent Bonn potential (CD-Bonn) and the Argonne V18 potential. In a comparison with the traditional approach of using the Miller-Spencer Jastrow correlations matrix elements for the $0\nu\beta\beta$ decay are obtained, which are larger in magnitude. We analyze the differences among various two-nucleon correlations including those of the unitary correlation operator method (UCOM) and quantify the uncertainties in the calculated $0\nu\beta\beta$ -decay matrix elements.

PACS numbers: 23.10.-s; 21.60.-n; 23.40.Bw; 23.40.Hc

Keywords: Neutrino mass; Neutrinoless double beta decay; Nuclear matrix element; Quasiparticle random phase approximation

I. INTRODUCTION

The present data on neutrino oscillations shows that pattern of neutrino masses and mixing (Pontecorvo-Maki-Nakagawa-Sakata mixing matrix) is not an analogue of that for quarks (Cabibbo-Kobayashi-Maskawa quark mixing matrix) [1, 2]. The generation of neutrino masses can be explored, if the absolute scale of neutrino masses will be fixed and the issue of leptonic CP violation will be understood [3]. This might happen, if the lepton number violating neutrinoless double beta decay ($0\nu\beta\beta$ -decay) will be undoubtable observed in running [4, 5] or planned [5, 6, 7, 8] $0\nu\beta\beta$ -decay experiments.

The $0\nu\beta\beta$ -decay is a very sensitive probe for the Majorana neutrino mass [7, 9, 10, 11, 12]. The $0\nu\beta\beta$ -decay can occur through different processes but all of them require that the neutrino has nonzero mass and is a Majorana particle [13]. The most proximate or discussed theoretical model is to mediate the $0\nu\beta\beta$ -decay by the exchange of a light Majorana neutrinos. A measurement of the decay rate, when combined with neutrino oscillation data and a reliable calculation of nuclear matrix elements (NMEs), would yield insight into all three neutrino mass eigenstates, the type of neutrino mass spectrum (normal hierarchy or inverted hierarchy) and possibly Majorana CP-violating phases.

An important subject in neutrino physics is a reliable calculation of the $0\nu\beta\beta$ -decay NME $M^{0\nu}$ [14]. Unfortunately, there are no observables that could be directly related to magnitudes of NMEs. The most popular nuclear structure methods, which has been applied for this task, are proton-neutron Quasiparticle Random Phase Approximation (QRPA) with its variants [15] and the Large-Scale Shell Model (LSSM) [16, 17, 18]. Recently, there has been significant progress towards the reduc-

tion of uncertainty in the calculated NMEs [15, 19]. A detailed anatomy of the $0\nu\beta\beta$ -decay NMEs pointed out a qualitative agreement between results of the QRPA-like and LSSM approaches [20, 21]. In particular, it was shown that only internucleon distances $r_{ij} \lesssim 2 - 3 \text{ fm}$ contribute to $M^{0\nu}$, what explains a small spread of results for different nuclei. Further, it has been shown that correlated NME uncertainties play an important role in the comparison of $0\nu\beta\beta$ -decay rates for different nuclei [22].

The improvement of the calculation of the nuclear matrix elements is a very important and challenging problem. The problem of the two-nucleon Short-Range Correlations (SRC) have recently inspired new $0\nu\beta\beta$ -decay studies [20, 21, 23]. In the majority of previous calculations SRC have been treated in a conventional way via Jastrow-type correlation function in the parametrization of Miller and Spencer [24]. Recently, it was found that the consideration of the unitary correlation operator method (UCOM) leads to increase of the $0\nu\beta\beta$ -decay NME by about 20-30% [20, 21, 23]. It was concluded that we do not know the best way to treat the SRC, a fact that contributes to uncertainties.

In the present article we improve on the Miller-Spencer Jastrow and the UCOM and perform a selfconsistent calculation of the $0\nu\beta\beta$ -decay NMEs by considering pairing, ground state and short-range correlations deduced from the same realistic nucleon-nucleon (NN) interaction. In particular, the two-nucleon short-range correlations will be determined within the *coupled cluster* or *exponential S* approach by using CD-Bonn and Argonne V18 NN-forces [26, 27] and compared with Jastrow and UCOM SRC. Then, they will be used in the QRPA and renormalized QRPA (RQRPA) calculations of the $0\nu\beta\beta$ -decay NMEs of experimental interest.

The paper is organized as follows: In Sec. II the formalism of the $0\nu\beta\beta$ -decay associated with exchange of light Majorana neutrinos is briefly reviewed. Sec. II is devoted to the analysis of different treatments of the two-nucleon short-range correlations in the context of the correlated $0\nu\beta\beta$ -decay operator. In Sec. IV we present numerical results for nuclei of experimental interest. Section V summarizes our findings.

II. FORMALISM

In this section we present basic expressions associated with the calculation of the $0\nu\beta\beta$ -decay NME, what allow us to discuss the effects of Finite Nucleon Size (FNS) and two-nucleon SRC.

By assuming the dominance of the light neutrino mixing mechanism the inverse value of the $0\nu\beta\beta$ -decay half-life for a given isotope (A, Z) is given by

$$\frac{1}{T_{1/2}} = G^{0\nu}(E_0, Z) |M'^{0\nu}|^2 |\langle m_{\beta\beta} \rangle|^2. \quad (1)$$

Here, $G^{0\nu}(E_0, Z)$ and $M'^{0\nu}$ are, respectively, the known phase-space factor (E_0 is the energy release) and the nuclear matrix element, which depends on the nuclear structure of the particular isotopes (A, Z), ($A, Z + 1$) and ($A, Z + 2$) under study. Under the assumption of the mixing of three light massive Majorana neutrinos the effective Majorana neutrino mass $\langle m_{\beta\beta} \rangle$ takes the form

$$\langle m_{\beta\beta} \rangle = \sum_i^N |U_{ei}|^2 e^{i\alpha_i} m_i, \quad (\text{all } m_i \geq 0), \quad (2)$$

where U_{ei} is the first row of the neutrino mixing matrix and the α_i are unknown Majorana phases. It is apparent that any uncertainty in $M'^{0\nu}$ makes the value of $\langle m_{\beta\beta} \rangle$ equally uncertain.

Our phase space factors $G^{0\nu}(E_0, Z)$, which include fourth power of axial-coupling constant $g_A = 1.25$, are tabulated in Ref. [28]. They agree quite closely with those given earlier in Ref. [29]. The $G^{0\nu}(E_0, Z)$ contain the inverse square of the nuclear radius (R_{nucl})⁻², compensated by the factor R_{nucl} in $M'^{0\nu}$. Different authors use different conventions for R_{nucl} ($R_{nucl} = r_0 A^{1/3}$ $r_0 = 1.2 \text{ fm}$ or $r_0 = 1.1 \text{ fm}$), a fact that is important to keep in mind when comparing the matrix elements without also looking at $G^{0\nu}(E_0, Z)$.

The nuclear matrix element $M'^{0\nu}$ is defined as

$$M'^{0\nu} = \left(\frac{g_A}{1.25} \right)^2 M^{0\nu}, \quad (3)$$

where $M^{0\nu}$ consists of Fermi, Gamow-Teller and tensor parts as

$$M^{0\nu} = -\frac{M_F}{g_A^2} + M_{GT} + M_T. \quad (4)$$

This definition of $M'^{0\nu}$ [15] allows to display the effects of uncertainties in g_A and to use the same phase factor $G^{0\nu}(E_0, Z)$ when calculating the $0\nu\beta\beta$ -decay rate.

In the QRPA (and RQRPA) $M^{0\nu}$ is written as sums over the virtual intermediate states, labeled by their angular momentum and parity J^π and indices k_i and k_f

$$\begin{aligned} M_K = & \sum_{J^\pi, k_i, k_f, \mathcal{J}} \sum_{pn p' n'} (-1)^{j_n + j_{p'} + J + \mathcal{J}} \times \\ & \sqrt{2\mathcal{J} + 1} \left\{ \begin{array}{ccc} j_p & j_n & J \\ j_{n'} & j_{p'} & \mathcal{J} \end{array} \right\} \times \\ & \langle p(1), p'(2); \mathcal{J} \parallel \mathcal{O}_K \parallel n(1), n'(2); \mathcal{J} \rangle \times \\ & \langle 0_f^+ \parallel [c_p^\dagger \widetilde{c}_{n'}]_J \parallel J^\pi k_f \rangle \langle J^\pi k_f \parallel J^\pi k_i \rangle \langle J^\pi k_f i \parallel [c_p^\dagger \widetilde{c}_n]_J \parallel 0_i^+ \rangle. \end{aligned} \quad (5)$$

The reduced matrix elements of the one-body operators $c_p^\dagger \widetilde{c}_n$ (\widetilde{c}_n denotes the time-reversed state) in the Eq. (5) depend on the BCS coefficients u_i, v_j and on the QRPA vectors X, Y [28]. The difference between QRPA and RQRPA resides in the way these reduced matrix elements are calculated.

The two-body operators $O_K, K = \text{Fermi (F), Gamow-Teller (GT), and Tensor (T)}$ in (5) contain neutrino potentials and spin and isospin operators, and RPA energies $E_{J^\pi}^{k_i, k_f}$:

$$\begin{aligned} O_F(r_{12}, E_{J^\pi}^k) &= \tau^+(1)\tau^+(2) H_F(r_{12}, E_{J^\pi}^k), \\ O_{GT}(r_{12}, E_{J^\pi}^k) &= \tau^+(1)\tau^+(2) H_{GT}(r_{12}, E_{J^\pi}^k) \sigma_{12}, \\ O_T(r_{12}, E_{J^\pi}^k) &= \tau^+(1)\tau^+(2) H_T(r_{12}, E_{J^\pi}^k) S_{12}. \end{aligned} \quad (6)$$

with

$$\begin{aligned} \mathbf{r}_{12} &= \mathbf{r}_1 - \mathbf{r}_2, \quad r_{12} = |\mathbf{r}_{12}|, \quad \hat{\mathbf{r}}_{12} = \frac{\mathbf{r}_{12}}{r_{12}}, \\ \sigma_{12} &= \vec{\sigma}_1 \cdot \vec{\sigma}_2 \\ S_{12} &= 3(\vec{\sigma}_1 \cdot \hat{\mathbf{r}}_{12})(\vec{\sigma}_2 \cdot \hat{\mathbf{r}}_{12}) - \sigma_{12}. \end{aligned} \quad (7)$$

Here, \mathbf{r}_1 and \mathbf{r}_2 are the coordinates of the nucleons undergoing beta decay.

The neutrino potentials are integrals over the exchanged momentum q ,

$$H_K(r_{12}, E_{J^\pi}^k) = \frac{2}{\pi} R \int_0^\infty f_K(qr_{12}) \frac{h_K(q^2) q dq}{q + E_{J^\pi}^k - (E_i + E_f)/2}, \quad (8)$$

The functions $f_{F,GT}(qr_{12}) = j_0(qr_{12})$ and $f_T(qr_{12}) = -j_2(qr_{12})$ are spherical Bessel functions.

The potentials (8) depend explicitly, though rather weakly, on the energies of the virtual intermediate states, $E_{J^\pi}^k$. The functions $h_K(q^2)$ that enter the H_K 's through the integrals over q in Eq. (8) are

$$\begin{aligned} h_F(q^2) &= g_V^2(q^2) \\ h_{GT}(q^2) &= \frac{g_A^2(q^2)}{g_A^2} \left[1 - \frac{2}{3} \frac{q^2}{q^2 + m_\pi^2} + \frac{1}{3} \left(\frac{q^2}{q^2 + m_\pi^2} \right)^2 \right] \end{aligned}$$

$$\begin{aligned}
& + \frac{2}{3} \frac{g_M^2(q^2)}{g_A^2} \frac{q^2}{4m_p^2}, \\
h_T(q^2) = & \frac{g_A^2(q^2)}{g_A^2} \left[\frac{2}{3} \frac{q^2}{q^2 + m_\pi^2} - \frac{1}{3} \left(\frac{q^2}{q^2 + m_\pi^2} \right)^2 \right] \\
& + \frac{1}{3} \frac{g_M^2(q^2)}{g_A^2} \frac{q^2}{4m_p^2} \quad (9)
\end{aligned}$$

Here, we used the Partially Conserved Axial Current (PCAC) hypothesis.

The FNS is taken into account via momentum dependence of the nucleon form-factors. For the vector, weak-magnetism and axial-vector form factors we adopt the usual dipole approximation as follows:

$$\begin{aligned}
g_V(q^2) &= \frac{g_V}{(1 + q^2/M_V^2)^2}, \\
g_M(q^2) &= (\mu_p - \mu_n) g_V(q^2), \\
g_A(q^2) &= \frac{g_A}{(1 + q^2/M_A^2)^2}, \quad (10)
\end{aligned}$$

where $g_V = 1$, $g_A = 1.00$ (quenched) and 1.25 (unquenched), $(\mu_p - \mu_n) = 3.70$. The parameters $M_V = 850 \text{ MeV}$ and $M_A = 1086 \text{ MeV}$ come from electron scattering and neutrino charged-current scattering experiments.

The $0\nu\beta\beta$ -decay matrix elements were usually calculated in some approximations, which are only partially justified (see also discussion in [15]):

i) The effect of higher order terms of nucleon currents was not taken into account. In this case we have

$$h_F(q^2) = g_V^2(q^2), \quad h_{GT}(q^2) = \frac{g_A^2(q^2)}{g_A^2}, \quad h_T(q^2) = 0. \quad (11)$$

We note that if in addition nucleons are considered to be point-like h_F and h_{GT} are equal to unity.

ii) The closure approximation for intermediate nuclear states was considered by replacing energies of intermediate states $[E_{J_\pi}^k - (E_i + E_f)/2]$ by an average value $\bar{E} \approx 10 \text{ MeV}$.

Within these approximations the neutrino potential in Eq. (8) can be written as [30]

$$\begin{aligned}
H_{bare}(r_{12}, \bar{E}) &= \frac{2}{\pi} \left[\sin(\bar{E}r_{12}) Ci(\bar{E}r_{12}) \right. \\
&\quad \left. - \cos(\bar{E}r_{12}) Si(\bar{E}r_{12}) \right] \frac{R_{nucl}}{r_{12}}. \quad (12)
\end{aligned}$$

Here, $Ci(x)$ and $Si(x)$ are the cosine and sine integrals, respectively. The value of \bar{E} has practically no impact on the behavior of neutrino exchange potential at short internucleon distances. In the limit $\bar{E} = 0$ and zero neutrino mass the neutrino potential is coulombic: $H_{bare}(r_{12}, \bar{E} = 0) = R_{nucl}/r_{12}$.

It is worth to mention some general properties of the Fermi M_F and the Gamow-Teller M_{GT} matrix elements,

in particular some multipole contributions of states of the intermediate odd-odd nucleus are equal to zero. We have

$$\begin{aligned}
M_F(J^+) &= 0 \quad \text{for odd } J, \\
M_F(J^-) &= 0 \quad \text{for even } J, \\
M_{GT}(0^+) &= 0. \quad (13)
\end{aligned}$$

III. SHORT RANGE CORRELATIONS FOR THE $0\nu\beta\beta$ -DECAY

An important component of the M_K in (5) is an unantisymmetrized two-body matrix element,

$$\langle p(1), p'(2); \mathcal{J} \parallel \mathcal{O}_K \parallel n(1), n'(2); \mathcal{J} \rangle, \quad (14)$$

constructed from two one-body matrix elements by coupling pairs of protons and neutrons to angular momentum \mathcal{J} . We note, in the closure approximation, i.e., if energies of intermediate states $(E_{J_\pi}^k - E_i)$ are replaced by an average value \bar{E} , and the sum over intermediate states is taken by closure, $\sum_n |J_k^\pi \rangle \langle J_k^\pi| = 1$, we end up with antisymmetrized two-body matrix elements. As the virtual neutrino has an average momentum of $\sim 100 \text{ MeV}$ [20], considerably larger than the differences in nuclear excitation, the closure approximation limit is found to be meaningful showing on the importance of correlations of the two β -decaying nucleons.

A. The Jastrow and UCOM short-range correlations

The QRPA (RQRPA) as well as the LSSM approaches do not allow to introduce short-range correlations into the two-nucleon relative wave function. The traditional way is to introduce an explicit Jastrow-type correlation function $f(r_{12})$ into the involved two-body transition matrix elements

$$\begin{aligned}
\langle \Psi_{\mathcal{J}} \parallel f(r_{12}) \mathcal{O}_K(r_{12}) f(r_{12}) \parallel \Psi_{\mathcal{J}} \rangle \\
\equiv \langle \bar{\Psi}_{\mathcal{J}} \parallel \mathcal{O}_K(r_{12}) \parallel \bar{\Psi}_{\mathcal{J}} \rangle. \quad (15)
\end{aligned}$$

Here,

$$\begin{aligned}
|\bar{\Psi}_{\mathcal{J}}\rangle &= f(r_{12}) |\Psi_{\mathcal{J}}\rangle, \\
|\Psi_{\mathcal{J}}\rangle &\equiv |n(1), n'(2); \mathcal{J}\rangle \quad (16)
\end{aligned}$$

are the relative wave function with and without the short-range correlations, respectively. In the parametrization of Miller and Spencer [24] we have

$$f(r_{12}) = 1 - e^{-ar^2} (1 - br^2), \quad a = 1.1 \text{ fm}^{-2}, \quad b = 0.68 \text{ fm}^{-2}. \quad (17)$$

These two parameters (a and b) are correlated and chosen in the way that the norm of the relative wave function $|\bar{\Psi}_{\mathcal{J}}\rangle$ is conserved.

Usually, the nuclear matrix element $M^{0\nu}$ is calculated in relative and center-of-mass coordinates as the Jastrow

correlation function depends only on r_{12} . This is achieved with help of the well-known Talmi-Moshinski transformation [31] for the harmonic oscillator basis. Within this procedure the chosen construction of the relative wave function, namely a product of $f(r_{12})$ with harmonic oscillator wave function in (16), is well justified. Any more complex structure of correlation function, e.g., a consideration of different correlation functions for different channels, would result in violation of requirements in (13) as the Talmi-Moshinski transformation is considered.

Recently, it was proposed [23] to adopt instead of the Jastrow method the UCOM approach for description of the two-body correlated wave function [25]. This approach describes not only short-range, but also central and tensor correlations explicitly by means of a unitary transformation. The state-independent short-range correlations are treated explicitly while long-range correlations should be described in a model space. Applied to a realistic NN interaction, the method produces a correlated interaction, which can be used as a universal effective interaction, for calculations within simple Hilbert spaces. The UCOM method produces good results for the binding energies of nuclei already at the Hartree-Fock level [32]. There are also some first applications for description of collective multipole excitations [33].

Within the UCOM the short-range and long-range correlations are imprinted into uncorrelated many body states by a unitary transformation. In the case of the $0\nu\beta\beta$ -decay calculation the correlated two-nucleon wave function was taken as

$$|\Psi_{\mathcal{J}}\rangle = C_r|\Psi_{\mathcal{J}}\rangle. \quad (18)$$

Here, C_r is the unitary correlation operator describing the short-range correlations. The explicit form of C_r is given in [25] with a separate parametrization for different LS-channels. In application to the $0\nu\beta\beta$ -decay this fact leads to a slight violation of conditions (13) when Talmi-Moshinski transformations are considered. The UCOM-corrected NMEs of the $0\nu\beta\beta$ -decay are significantly less suppressed when compared with those calculated with Jastrow SRC [20, 23].

B. Self-consistent two-body short-range correlations

The two-nucleon wave function with short range correlations can be calculated from the same realistic NN-interaction, which is used in the derivation of the Brueckner G-matrix elements of the nuclear Hamiltonian. A method of choice is, e.g., the Brueckner-Bethe hole-line expansion, the coupled cluster method (CCM) or exponential S approach and the approach of self-consistent evaluation of Green functions [26].

There are various modern NN potentials, which yield a very accurate fit to the nucleon-nucleon scattering phase shifts. Two of them are the so-called charge-dependent

Bonn potential (CD-Bonn) [34] and the Argonne V18 potential (Argonne) [35]. They differ in description of both long-range and short-range parts of NN-interaction. The CD-Bonn is derived in the framework of the relativistic meson field theory. The Argonne potential is a purely local potential in the sense that it uses the local form of the one-pion exchange potential for the long-range part and parametrizes the contributions of medium and short-range distances in terms of local functions multiplied by a set of spin-isospin operators.

We have chosen the CCM [27] to evaluate the effect of short-range correlation on the $0\nu\beta\beta$ -decay NMEs, because it provides directly correlated two-body wave functions. The basic features of the CCM are described in the review article by Kümmel [37]. The developments of this many-body approach with applications can be found in [38, 39].

The CCM starts by assuming an appropriate Slater determinant $|\Phi\rangle$ as a first approximation for the exact eigenstate of the A-particle system. The many-body wave function of the coupled cluster or exp(S) method can be written as

$$|\Phi\rangle_{corr.} = exp\left(\sum_{n=1}^A \hat{S}_n\right) |\Phi\rangle. \quad (19)$$

The n-particle n-hole excitation operator \hat{S}_n is given by

$$\hat{S}_n = \frac{1}{(n!)^2} \times \sum_{\nu_i, \rho_i} \langle \rho_1 \dots \rho_n | S_n | \nu_1 \dots \nu_n \rangle a_{\rho_1}^\dagger \dots a_{\rho_n}^\dagger a_{\nu_n} \dots a_{\nu_1}. \quad (20)$$

The sum in (20) is restricted to states ρ_i which are unoccupied in the model state $|\Phi\rangle$, while states ν_i refer to states which are occupied in $|\Phi\rangle$.

A Slater determinant of harmonic oscillator wave functions is considered for $|\Phi\rangle$. For a given nuclear system of interest an appropriate value of the oscillator length b is chosen. In the so-called S_2 approximation of the CCM the amplitudes defining \hat{S}_n with $n > 3$ in (19) are ignored. This means that effects beyond Hartree-Fock and two-body correlations (i.e. genuine three- and more-particle correlations) are ignored. This leads to a coupled set of equations for the evaluation of the correlation operators \hat{S}_1 and \hat{S}_2 [27]. Therefore this S_2 approximation corresponds essentially to the Brueckner-Hartree-Fock (BHF) approximation of the hole-line expansion or Brueckner theory. In fact, the hole-hole scattering terms, which are included in the S_2 but ignored in BHF turn out to yield small effects only. Therefore it is consistent to combine the correlation effects from CCM with the matrix elements of the G-matrix, the effective interaction determined in the BHF approximation.

The use of the oscillator ansatz in Slater determinant $|\Phi\rangle$ in eq.(19) leads to an evaluation of the correlated

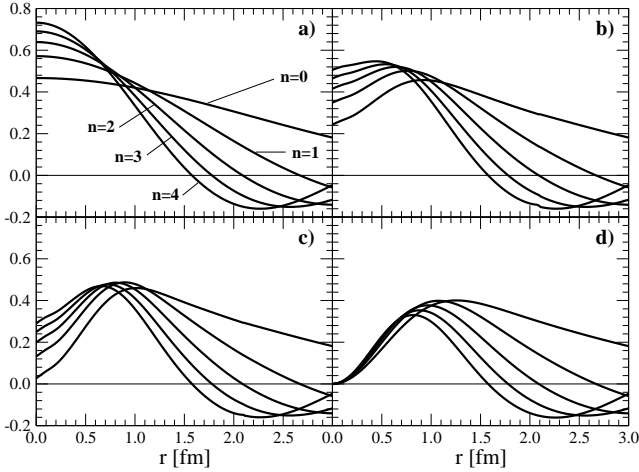


FIG. 1: Two nucleon wave functions as a function of the relative distance for the 1S_0 partial wave and radial quantum numbers $n = 0, 1, 2, 3$ and 4 . The results in panel a) are for uncorrelated two-nucleon wave functions. The results in panels b), c) and d), respectively, are with coupled cluster method with CD-Bonn potential, coupled cluster method with Argonne potential and Miller-Spencer Jastrow short-range correlations. The harmonic oscillator parameter b is $2.18 fm$.

two-nucleon wave functions in terms of product wave functions for the relative and center-of-mass coordinates. The two-body states take the form

$$|[n(lS)j]NL\mathcal{J}\tau\rangle. \quad (21)$$

Here, N and L denote the harmonic-oscillator quantum numbers for the center of mass wave function and l refers to the orbital angular momentum for the relative motion, which is coupled with a total spin of the pair S to angular momentum \mathcal{J} . The basis states for the radial part of this relative motion are labeled by a quantum number n .

As an example we present in Fig. 1 relative wave functions for correlated and uncorrelated two-body wave functions in the case of 1S_0 partial waves and different values of the radial quantum numbers n ($n = 0, 1, 2, 3$ and 4). In panel a) uncorrelated harmonic oscillator wave functions are plotted. Panels b) and c) show the relative wave functions obtained with help of CCM employing the CD-Bonn and the Argonne potentials. For a comparison relative wave functions with Miller-Spencer Jastrow SRC are displayed in panel d). While the Jastrow ansatz suppresses the relative wave function in the limit $r_{12} \rightarrow 0$ completely, we find that this suppression effect is much weaker in the CCM calculation. This is true even if the Argonne potential is used, which is known to produce stronger short-range components than the softer CD-Bonn potential. Also note that the correlated wave functions derived from realistic interactions exhibit a short-range behavior which depends on the radial quantum number n , whereas the Jastrow approach yields almost identical relative wave functions for small values of r_{12} .

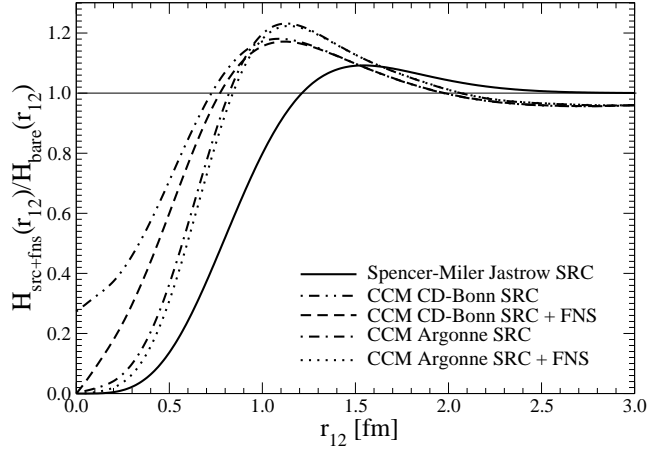


FIG. 2: The ratio of neutrino potentials with and without two-nucleon short-range correlations (SRC). Results are shown for the CCM CD-Bonn and Argonne and Miller-Spencer SRC with and without consideration of the effect of finite size of a nucleon. It is assumed $\bar{E} = 8 MeV$.

components of the NN interaction at short distances are weaker for the CD-Bonn potential in comparison with Argonne interaction. But, in the case of the Jastrow SRC the reduction of the relative wave function for small values of r_{12} is even much stronger.

The advantage of the CCM [27] is a factorization of the correlated two-body wave function on a product of a correlation function and a harmonic oscillator wave function. This allows us to discuss the effect of the SRC in terms of the correlated operator, which is a product of the transition operator $\mathcal{O}_K(r_{12})$ and two correlation functions $f(r_{12})$ (see Eqs. (15)). For our purposes we consider CCM CD-Bonn f_B and CCM Argonne f_A correlation functions deduced from the $^1S_0(n=0)$ correlated two-body wave function. The use of this single correlation function for all partial waves and quantum numbers n is numerically well justified and is dictated by the use of the Talmi-Moshinski transformation in the evaluation of the $0\nu\beta\beta$ -decay matrix element.

In Fig. 2 the differences between the CCM and the Miller-Spencer SRC are manifested by plotting the ratio of correlated $H_{src+fns}(r_{12})$ and uncorrelated $H_{bare}(r_{12})$ neutrino potentials. The averaged energy of intermediate nuclear states \bar{E} is $8 MeV$. For sake of simplicity the effect of higher order terms of nucleon currents on the neutrino potential is neglected. From Fig. 2 we see that there is a significant difference between the CCM and the Miller-Spencer treatment of the SRC. The maxima of the CCM and the Spencer-Miller curves occur at $1 fm$ and $1.5 fm$, respectively. One finds also that the reduction at short distances is much weaker for CD-Bonn than for Argonne interactions.

For purpose of numerical calculation of the $0\nu\beta\beta$ -decay NMEs we present the CCM short-range correlation functions in an analytic form of Jastrow-like function as

$$f_{A,B}(r_{12}) = 1 - c e^{-ar^2} (1 - br^2). \quad (22)$$

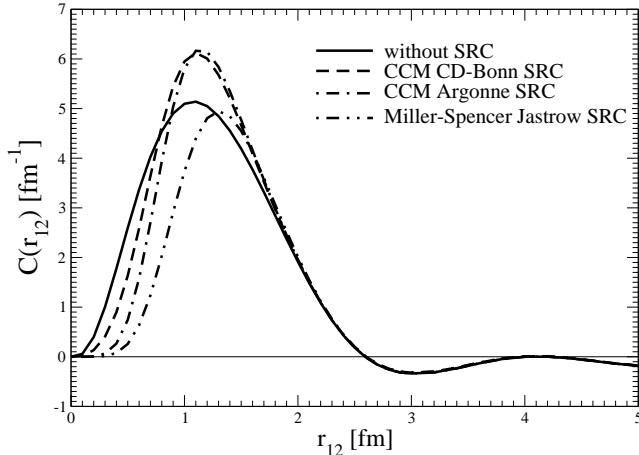


FIG. 3: The r_{12} dependence of $M^{0\nu}$ in ^{76}Ge evaluated in the model space that contains twelve subshells. The four curves show the effects of different treatment of short-range correlations (SRC). The finite nucleon size (FNS) is taken into account.

The set of parameters for Argonne and CD-Bonn NN interactions is given by

$$\begin{aligned} f_A(r_{12}) : a &= 1.59 \text{ fm}^{-2}, \quad b = 1.45 \text{ fm}^{-2}, \quad c = 0.92, \\ f_B(r_{12}) : a &= 1.52 \text{ fm}^{-2}, \quad b = 1.88 \text{ fm}^{-2}, \quad c = 0.46. \end{aligned} \quad (23)$$

The calculated NMEs with these short-range correlation functions agree within a few percentages with those obtained without this approximation. We note that the dependence of the SRC on the value of oscillator length b is rather weak.

In Fig. 3 the r_{12} dependence of $M^{0\nu}$ is shown for CCM Argonne, CCM CD-Bonn and phenomenological Jastrow SRC for the $0\nu\beta\beta$ -decay of ^{76}Ge . The quantity $C(r_{12})$ is defined by

$$M^{0\nu} = \int_0^\infty C(r_{12}) dr_{12}. \quad (24)$$

We note that the range of r_{12} is practically restricted from above by $r_{12} \leq 2R_{nucl}$. From the Fig. 3 we see that a modification of the neutrino potential due to the different types of SRC is transmitted to the behavior of $C(r_{12})$ for $r_{12} \leq 2 \text{ fm}$. Both, the CCM short-range correlation functions (see Fig. 2) and $C(r_{12})$ with SRC switched off (but with FNS effect) have maxima for $r_{12} \simeq 1 \text{ fm}$ unlike the phenomenological Jastrow function with maximum shifted to $r_{12} = 1.5 \text{ fm}$. This explains a significant increase of $C(r_{12})$ with CCM SRC and suppression of $C(r_{12})$ with Jastrow SRC in this region. This phenomenon clarifies also why the values of $M^{0\nu}$ obtained with CCM SRC are comparable to those calculated when only the FNS effect is considered (see Table I). The increase of $C(r_{12})$ for $r_{12} \simeq 1 \text{ fm}$ compensates its reduction in the range $r_{12} \leq 0.7 \text{ fm}$.

C. Finite nucleon size and two-body short range correlations

The FNS effects are introduced in the calculation of the $0\nu\beta\beta$ -decay NMEs by the dipole form factors in momentum space. The form factor simulates the fact that nucleon is not a point particle, and therefore as q^2 increases, the probability that nucleon will stay intact (and not produce pions etc) decreases. The physics of FNS and SRC is different, but both reduce the magnitude of the operator when q^2 increases or equivalently r_{12} decreases. It was found [20] that Miller-Spencer and the UCOM short-range correlations essentially eliminate the effect of the FNS on the matrix elements. The same is expected to be valid also for the CCM CD-Bonn and Argonne short-range correlations. From Fig. 2 we see that the ratio of correlated and uncorrelated neutrino potentials is changed only weakly if in addition to two-nucleon SRC the effect of the FNS is taken into account.

It is worth mentioning that the behavior of the UCOM correlated neutrino potential differs strongly from those calculated with the CCM and Jastrow SRC. This is manifested in Fig. 4. The studied ratio of UCOM correlated and uncorrelated neutrino potentials never exceeds unity unlike in the case of CCM correlations (see Fig. 2). Actually, the UCOM SRC imitate the effect of the FNS with form-factor cut-off of about 850 MeV. The two-nucleon wave function can be treated as two point-like objects for nucleon separations greater than about 1.5 fm.

The effect of the SRC on the $0\nu\beta\beta$ -decay NMEs has been referred mostly to case when the FNS is taken into account. It was found that Miller-Spencer SRC reduces the $0\nu\beta\beta$ -decay NMEs by 20-30% and UCOM SRC by $\sim 5\%$ [20]. For better understanding of this effect we calculate the $0\nu\beta\beta$ -decay of ^{76}Ge , ^{100}Mo and ^{130}Te with and without consideration of the FNS. The 12 levels (^{76}Ge) and 13 levels (^{100}Mo and ^{130}Te) single particle model spaces are used in calculation. The results are displayed in Table I. The bare NME was obtained in the limit of cut-off masses $M_{V,A}$ go to infinity and with the two-nucleon SRC switched off. The FNS values of $M^{0\nu}$ are determined by nucleon form factors with phenomenological values of M_V and M_A . We see that the FNS reduces $M^{0\nu}$ by 20%. The $0\nu\beta\beta$ -decay NME is suppressed by about 20-30% and 40-50% in the cases of the two-nucleon CCM (Argonne potential) and the phenomenological Miller-Spencer SRC, respectively. It is also shown that once SRC effects are included the consideration of the nucleon form-factors almost does not influence the value of $M^{0\nu}$. It is because the FNS and the SRC effects act coherently on the $0\nu\beta\beta$ -decay NMEs and both diminish them. However, the effect of the SRC is at least partially stronger (CCM SRC) or stronger (Miller-Spencer SRC) in comparison with the FNS effect.

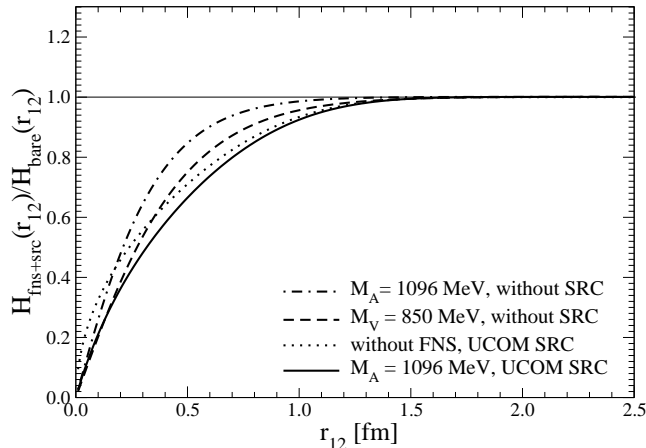


FIG. 4: A ratio of neutrino potentials with inclusion of the finite nucleon size effect (FNS) and bare neutrino potential for cut-off masses M_V and M_A . This is compared with ratio of neutrino potential with UCOM short range correlations (SRC) and bare neutrino potential. $E = 8 \text{ MeV}$ is used in calculation.

IV. NUMERICAL RESULTS

The nuclear matrix elements of the $0\nu\beta\beta$ -decay of the experimentally interesting nuclei $A = 76, 82, 96, 100, 116, 128, 130$ and 136 are systematically evaluated using the QRPA and RQRPA. In the present calculations, we improve on the Miller-Spencer Jastrow and UCOM methods by engaging the SRC calculated within the exp(S) approach with the CD-Bonn and Argonne V18 NN interactions. This allows a consistent study of the $0\nu\beta\beta$ -decay NMEs as for the first time the same realistic nucleon-nucleon force is used for the description of the pairing interactions, RPA ground state correlations and the two-nucleon SRC.

The nuclear structure calculations are performed as described in our previous publications [15, 19, 20]. Three different single-particle model spaces are used: small (2-3 oscillator shells), intermediate (3-4 oscillator shells) and large (5 oscillator shells) model spaces (see Ref. [19]). The single-particle energies are obtained by using a Coulomb-corrected Woods-Saxon potential [41]. The interactions employed are the Brueckner G-matrices which are a solution of the Bethe-Goldstone equation with the CD-Bonn and Argonne V18 one-boson exchange potentials. The pairing two-body interaction is fitted in the standard way and the pairing parameters of the BCS are adjusted to reproduce the phenomenological pairing gaps, extracted from the atomic mass tables. We renormalize the particle-particle and particle-hole channels of the G-matrix interaction of the nuclear Hamiltonian by introducing the parameters g_{pp} and g_{ph} , respectively. We use $g_{ph} = 1$ throughout what allows to reproduce well the available data on the position of the giant Gamow-Teller resonance. The particle-particle strength parameter g_{pp} of the (R)QRPA is fixed by the data on the two-neutrino

double beta decays.

The NME calculated within the above procedure, which includes three different model spaces, is denoted as the averaged $0\nu\beta\beta$ -decay NME $\langle M^{0\nu} \rangle$. The results are presented separately for the CD-Bonn and Argonne interactions and for two different values of the axial coupling constant g_A in Table II. We confirm again that with considered procedure the $0\nu\beta\beta$ -decay values become essentially independent on the size of the single-particle basis and rather stable with respect to the possible quenching of the g_A . The NMEs obtained with the CD-Bonn NN interaction are slightly larger as those calculated with the Argonne interaction. This is explained by the fact that the CCM Argonne correlation function cuts out more the small r_{12} part from the relative wave function of the two-nucleons as the CCM CD-Bonn correlation function. The differences in NMEs due to a different treatment of the SRC do not exceed differences between the QRPA and the RQRPA results.

In Table III we show the calculated ranges of the nuclear matrix element $M^{0\nu}$ evaluated within the QRPA and RQRPA, with standard ($g_A = 1.254$) and quenched ($g_A = 1.0$) axial-vector couplings and with the CCM CD-Bonn and Argonne SRC functions. These ranges quantify the uncertainty in the calculated $0\nu\beta\beta$ -decay NMEs. In respect to the central value their accuracy is of the order of 25%. A significant amount of the uncertainty is due to a quenching of the axial-vector coupling constant g_A in nuclear medium [42]. For a comparison we present also the NMEs calculated with the phenomenological Jastrow SRC function in Table III. The notable differences between the results calculated with Jastrow and CCM SRC are about of 20-30%. Of course, the results obtained with the CCM SRC are preferable. Unfortunately, they can not be directly compared to those of the complementary Large-Scale Shell Model (LSSM) as they have been evaluated only with the Jastrow and UCOM SRC and for $g_A = 1.25$ [18, 21]. It is reasonable to assume that the LSSM values (see Table III) would be increased also by the order of 20-30%, if the CCM SRC would be considered. Recall, that within both approaches qualitatively the same r_{12} dependence of $M^{0\nu}$ was found [20, 21]. Fig. 5 shows our calculated ranges for $M^{0\nu}$, which are compared with ranges calculated with Miller-Spencer Jastrow function and the latest LSSM results. Given the interest in the subject, we show the range of predicted half-lives corresponding to our full range of $M^{0\nu}$ in Table III.

Recently, the occupation numbers of neutron and proton valence orbits in the ^{76}Ge and ^{76}Se nuclei were measured by neutron and proton adding and removing transfer reactions [43, 44]. In following theoretical study [45] these results were used as a guideline for modification of the effective mean field energies that results in better description of these quantities. The calculation of the $0\nu\beta\beta$ -decay NME for ^{76}Ge performed with adjusted mean field [45] and in combination with the selfconsistent RQRPA (SRQRPA) method [46], which conserves the mean particle number in correlated ground state, lead to

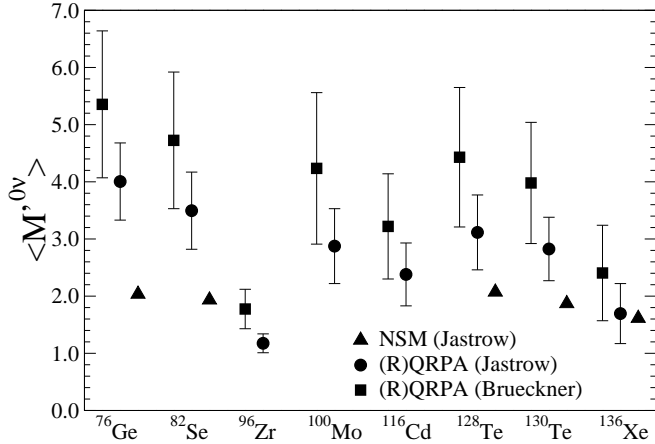


FIG. 5: The full ranges of $M^{0\nu}$ with the CCM and Miller-Spencer Jastrow treatments of the short range correlations. For comparison the results of a recent Large Scale Shell Model evaluation of $M^{0\nu}$ that used the Jastrow-type treatment of short range correlations are also shown.

a reduction of $M^{0\nu}$ by 25% when compared to previous QRPA value. The phenomenological Jastrow and UCOM SRC were considered. We found that a reduction of 20% in the case of CCM CD-Bonn SRC. We have

$$\begin{aligned}
 \langle M^{0\nu} \rangle &= 4.24(0.44), \quad 3.49(0.23), \quad \text{Jastrow} \\
 &= 5.19(0.54), \quad 4.60(0.23), \quad \text{UCOM} \\
 &= 6.32(0.32), \quad 5.15(0.44), \quad \text{CCM}.
 \end{aligned}
 \tag{25}$$

Here, the first and second values in each line correspond to the QRPA with Woods-Saxon mean field and the SRQRPA with adjusted Woods-Saxon mean field [45] way of calculations, respectively. In order to better understand the role of proton and neutron occupation numbers in the $0\nu\beta\beta$ -decay calculation further experimental and theoretical studies are needed what goes beyond the scope of this paper.

V. CONCLUSIONS

We have addressed the issue of a consistent treatment of the short-range correlations in the context of

the $0\nu\beta\beta$ -decay. These correlations, which have origin in the short-range repulsion of the realistic NN interaction, are neglected in the mean-field, the LSSM and the QRPA descriptions. Till now, Miller-Spencer Jastrow and the UCOM SRC have been introduced into the involved two-body transition matrix elements, changing two neutrons into two protons, to achieve healing of the correlated wave functions. The effect of these SRC was considered as an uncertainty [20].

In this article the CCM short-range correlations has been considered. They were obtained as a solution of the coupled cluster method with realistic CD-Bonn and Argonne V18 interactions. An analysis of the squared correlation functions, represented by a ratio of correlated and uncorrelated neutrino potentials, has showed a principal differences among the Miller-Spencer, UCOM and CCM SRC. In addition, the importance of the effect of the FNS was studied. It was found that both CCM SRC and the FNS effect reduces the $0\nu\beta\beta$ -decay NMEs by a comparable amount for a considered choice of form-factor masses. The suppression due to Miller-Spencer SRC is about twice larger when compared to results without SRC and the FNS effect.

Finally, we have improved the presently available calculations by performing a consistent calculation of the $0\nu\beta\beta$ -decay NMEs in which pairing, ground-state correlations and the short-range correlations originate from the same realistic NN interaction, namely from the CD-Bonn and Argonne potentials.

Acknowledgments

Discussions with Petr Vogel are gratefully acknowledged. We acknowledge the support of the EU ILIAS project under the contract RII3-CT-2004-506222, the Deutsche Forschungsgemeinschaft (436 SLK 17/298), the Transregio Project TR27 "Neutrinos and Beyond" and, in addition, F.Š was supported by the VEGA Grant agency of the Slovak Republic under the contract No. 1/0639/09.

[1] G. L. Fogli, E. Lisi, A. Marrone and A. Palazzo, *Progr. Part. Nucl. Phys.* **57**, 742 (2006).
 [2] M. Maltoni, Th. Schwetz, hep-ph/0812.3161.
 [3] S.M. Bilenky, C. Giunti, J.A. Grifols, E. Massó, *Phys. Rep.* **379**, 69 (2003).
 [4] NEMO Collaboration, R. Arnold *et al.*, *Phys. Rev. Lett.* **95**, 182302 (2005); *Nucl. Phys. A* **765**, 483 (2006).
 [5] CUORE Collaboration, C. Arnaboldi *et al.*, *Phys. Lett.*

B **584**, 260 (2004); A. Guliani, *J. Phys. Conf. Ser.* **120**, 052051 (2008).
 [6] GERDA Collaboration, Abt I *et al.*, arXiv:0404039[hep-ex]; H. Simgen, *J. Phys. Conf. Ser.* **120**, 052052 (2008).
 [7] Frank T. Avignone III, Steven R. Elliott, and Jonathan Engel, *Rev. Mod. Phys.* **80**, 481 (2008).
 [8] A.S. Barabash, *Phys. Atom. Nucl.* **70**, 1191 (2007).
 [9] A. Faessler and F. Šimkovic, *J. Phys. G* **24**, 2139 (1998).

- [10] J.D. Vergados, Phys. Rep. **361**, 1 (2002).
- [11] S. R. Elliott and P. Vogel, Annu.Rev.Nucl.Part.Sci. **52**,115(2002); S.R. Elliott, Nucl. Phys. Proc. Suppl. **138**, 275 (2005).
- [12] S. R. Elliott and J. Engel, J. Phys. G **30**, R183 (2004).
- [13] J. Schechter and J.W.F. Valle, Phys. Rev. D **25**, 2951 (1982); M. Hirsch, H.V. Klapdor-Kleingrothaus, S. Kovalenko, Phys. Lett. B **372**, 8 (1996).
- [14] K. Zuber, arXiv:0511009[nucl-ex].
- [15] V.A. Rodin, A. Faessler, F. Šimkovic and P. Vogel, Nucl. Phys. **A766**, 107 (2006) and erratum, Nucl. Phys. **A793**, 213 (2007).
- [16] E. Caurier, F. Nowacki, A. Poves, J. Retamosa, Phys. Rev. Lett. **77**, 1954 (1996).
- [17] E. Caurier, F. Nowacki, A. Poves, Eur. Phys. J. A **36**, 195 (2008).
- [18] E. Caurier, J. Menéndez, F. Nowacki, A. Poves, Phys. Rev. Lett. **100** 052503 (2008).
- [19] V.A. Rodin, A. Faessler, F. Šimkovic and P. Vogel, Phys. Rev. C **68**, 044302 (2003).
- [20] F. Šimkovic, A. Faessler, V.A. Rodin, P. Vogel, and J. Engel, Phys. Rev. C **77**, 045503 (2008).
- [21] J. Menendez, A. Poves, E. Caurier, F. Nowacki, arXiv:0801.3760[nucl-th].
- [22] A. Faessler, G.L. Fogli, E. Lisi, V. Rodin, A.M. Rotunno, F. Šimkovic, arXiv:0810.5733[hep-ph].
- [23] M. Kortelainen, O. Civitarese, J. Suhonen, and J. Toivanen, Phys. Lett. **B647**, 128 (2007); M. Kortelainen and J. Suhonen, Phys. Rev. C **75**, 051303(R) (2007); M. Kortelainen and J. Suhonen, arXiv:0708:0115.
- [24] G. A. Miller and J. E. Spencer, Ann. Phys. **100**, 562 (1976).
- [25] H. Feldmeier, T. Neff, R. Roth and J. Schnack, Nucl. Phys. A **632**, 61 (1998); T. Neff and H. Feldmeier, Nucl. Phys. A **713**, 311 (2003); R. Roth, T. Neff, H. Hergert, and H. Feldmeier, Nucl. Phys. A **745**, 3 (2004).
- [26] H. Mütter and A. Polls, Phys. Rev. C **61**, 014304 (1999); Prog. Part. Nucl. Phys. **45**, 243 (2000).
- [27] C. Giusti, H. Mütter, F.D. Pacati, and M. Stauf, Phys. Rev. C **60**, 054608 (1999).
- [28] F. Šimkovic, G. Pantis, J.D. Vergados, and A. Faessler, Phys. Rev. C **60**, 055502 (1999).
- [29] F. Boehm and P. Vogel, *Physics of Massive Neutrinos* 2nd ed., Cambridge Univ. Press, Cambridge, 1992.
- [30] T. Tomoda, Rep. Prog. Phys. **54**, 53 (1991).
- [31] I. Talmi, Helv Phys. Acta **25**, 185 (1952); M. Moshinski, Nucl. Phys. **13**, 104 (1959).
- [32] R. Roth, H. Hergert, P. Papakonstantinou, T. Neff and H. Feldmeier, Phys. Rev. C **72**, 034002 (2005).
- [33] N. Paar, P. Papakonstantinou, H. Hergert, and R. Roth, Phys. Rev. C **74**, 014318 (2006).
- [34] S. Machleidt, F. Sammarruca, and Y. Song, Phys. Rev. C **53**, R1483 (1995).
- [35] R.B. Wiringa, V.G.J. Stoks, and R. Schiavilla, Phys. Rev. C **51**, 38 (1995).
- [36] F. Coester, Nucl. Phys. **7**, 421 (1958); F. Coester and H. Kümmel, Nucl. Phys. **17**, 477 (1960).
- [37] H. Kümmel, K.H. Lührmann, and J.G. Zabolitsky, Phys. Rep. **36**, 1 (1978).
- [38] R.F. Bishop, in *Microscopic Quantum Many-Body Theories and Their Applications*, edited by J. Navarro and A. Polls (Springer, Berlin, 1998).
- [39] B. Mihaila and J.H. Heisenberg, Phys. Rev. C **61**, 054309 (2000).
- [40] D.J. Dean and M. Hjorth-Jensen, Phys. Rev. C **69**, 054320 (2004).
- [41] A. Bohr and B. Mottelson Nuclear Structure, Vol. I, V. J. Benjamin, New York, 1969.
- [42] A. Faessler, G.L. Fogli, E. Lisi, V. Rodin, A.M. Rotunno, F. Šimkovic, J. Phys. G **35**, 075104 (2008).
- [43] J.P.Schiffer et al., Phys. Rev. Lett. **100**, 112501 (2008).
- [44] B.P. Kay et al., arXiv:0810.4108[nucl-ex].
- [45] F. Šimkovic, A. Faessler, and P. Vogel, arXiv:0812.0348[nucl-th].
- [46] D.S. Delion, J. Dukelsky, and P. Schuck, Phys. Rev. C **55**, 2340 (1997); F. Krmpotić et al., Nucl. Phys. A **637**, 295 (1998).

TABLE I: Nuclear matrix elements for the $0\nu\beta\beta$ -decays of ^{76}Ge , ^{100}Mo and ^{136}Te within the QRPA. The results are presented: i) (bare) no correlations and no nucleon form factors; ii) (FNS) no correlations but with nucleon form factors; iii) (SRC) CCM Argonne and Miller-Spencer short-range correlations but without nucleon form factors; iv) (FNS+SRC) correlations and nucleon form factors.

Nucleus	bare	FNS	SRC		FNS + SRC	
			CCM	Miller-Spencer	CCM	Miller-Spencer
$^{76}\text{Ge} \rightarrow ^{76}\text{Se}$	7.39	6.14	5.86	4.46	5.91	4.54
$^{100}\text{Mo} \rightarrow ^{100}\text{Ru}$	6.15	4.75	4.40	2.87	4.46	2.96
$^{130}\text{Te} \rightarrow ^{130}\text{Xe}$	5.62	4.49	4.22	2.97	4.27	3.04

TABLE II: Averaged $0\nu\beta\beta$ nuclear matrix elements $\langle M^{0\nu} \rangle$ and their variance σ (in parentheses) calculated within the RQRPA and the QRPA. The pairing and residual interactions of the nuclear Hamiltonian and the two-nucleon short-range correlations (SRC) are derived from the same realistic nucleon-nucleon interaction (CD-Bonn and Argonne potentials) by exploiting the Brueckner-Hartree-Fock and coupled cluster (CCM) methods. Three sets of single particle level schemes are used, ranging in size from 9 to 23 orbits. The strength of the particle-particle interaction is adjusted so the experimental value of the $2\nu\beta\beta$ -decay nuclear matrix element M_{GT}^{exp} is correctly reproduced. Both free nucleon ($g_A = 1.254$) and quenched ($g_A = 1.0$) values of axial-vector coupling constant are considered.

Nuclear transition	g_A	M_{GT}^{exp} [MeV $^{-1}$]	$\langle M^{0\nu} \rangle$		$\langle M^{0\nu} \rangle$	
			CCM CD-Bonn SRC		CCM Argonne SRC	
			RQRPA	QRPA	RQRPA	QRPA
$^{76}\text{Ge} \rightarrow ^{76}\text{Se}$	1.25	0.15	5.44(0.23)	6.32(0.32)	4.97(0.19)	5.81(0.27)
	1.00	0.23	4.62(0.22)	5.16(0.25)	4.21(0.14)	4.77(0.20)
$^{82}\text{Se} \rightarrow ^{82}\text{Kr}$	1.25	0.10	4.86(0.20)	5.65(0.27)	4.44(0.19)	5.19(0.24)
	1.00	0.16	3.93(0.15)	4.48(0.20)	3.67(0.14)	4.19(0.18)
$^{96}\text{Zr} \rightarrow ^{96}\text{Mo}$	1.25	0.11	2.01(0.20)	2.09(0.03)	1.84(0.16)	1.90(0.09)
	1.00	0.17	1.72(0.15)	1.93(0.11)	1.55(0.12)	1.74(0.11)
$^{100}\text{Mo} \rightarrow ^{100}\text{Ru}$	1.25	0.22	4.28(0.28)	5.25(0.31)	3.85(0.31)	4.75(0.33)
	1.00	0.34	3.44(0.19)	4.07(0.22)	3.14(0.23)	3.69(0.25)
$^{116}\text{Cd} \rightarrow ^{116}\text{Sn}$	1.25	0.12	3.41(0.24)	3.99(0.15)	3.06(0.22)	3.54(0.27)
	1.00	0.19	2.68(0.19)	3.03(0.19)	2.47(0.17)	2.74(0.21)
$^{128}\text{Te} \rightarrow ^{128}\text{Xe}$	1.25	0.034	4.82(0.15)	5.49(0.16)	4.32(0.16)	4.93(0.16)
	1.00	0.053	3.67(0.11)	4.16(0.12)	3.32(0.11)	3.77(0.12)
$^{130}\text{Te} \rightarrow ^{130}\text{Xe}$	1.25	0.036	4.40(0.13)	4.92(0.12)	3.91(0.14)	4.37(0.14)
	1.00	0.056	3.38(0.08)	3.77(0.07)	3.02(0.10)	3.38(0.10)
$^{136}\text{Xe} \rightarrow ^{136}\text{Ba}$	1.25	0.030	2.89(0.17)	3.11(0.13)	2.59(0.16)	2.78(0.13)
	1.00	0.045	2.26(0.11)	2.42(0.08)	2.03(0.10)	2.17(0.09)
	1.25	0	2.53(0.17)	2.73(0.13)	2.25(0.16)	2.43(0.13)
	1.00	0	1.87(0.11)	2.01(0.08)	1.67(0.10)	1.80(0.09)

TABLE III: The calculated ranges of the nuclear matrix element $M'^{0\nu}$ evaluated within the QRPA and RQRPA, with standard ($g_A = 1.254$) and quenched ($g_A = 1.0$) axial-vector couplings and with coupled cluster method (CCM) CD-Bonn and Argonne short-range correlation (SRC) functions. Column 4 contains the ranges of $M'^{0\nu}$ with the phenomenological Miller-Spencer Jastrow treatment of short range correlations, while column 6 shows the CCM SRC-based results. For comparison the recent results of a large scale shell model (LSSM) evaluation of $M'^{0\nu}$ [18] that used the Miller-Spencer Jastrow SRC and $g_A = 1.25$ are given in column 2. However, they have to be scaled by factor (1.1 fm/1.2 fm) as different value of r_0 ($R_{nucl} = r_0 A^{1/3}$) was considered. Columns 3, 5 and 7 give the $0\nu\beta\beta$ -decay half-lives or half-life ranges corresponding to values of the matrix-elements in columns 2, 4 and 6 for $\langle m_{\beta\beta} \rangle = 50$ meV.

Nucleus	LSSM (Jastrow SRC)		(R)QRPA (Jastrow SRC)		(R)QRPA (CCM SRC)	
	$M'^{0\nu}$	$T_{1/2}^{0\nu} (\langle m_{\beta\beta} \rangle = 50 \text{ meV})$	$M'^{0\nu}$	$T_{1/2}^{0\nu} (\langle m_{\beta\beta} \rangle = 50 \text{ meV})$	$M'^{0\nu}$	$T_{1/2}^{0\nu} (\langle m_{\beta\beta} \rangle = 50 \text{ meV})$
^{76}Ge	2.22	3.18×10^{27}	(3.33, 4.68)	$(6.01, 11.9) \times 10^{26}$	(4.07, 6.64)	$(2.99, 7.95) \times 10^{26}$
^{82}Se	2.11	7.93×10^{26}	(2.82, 4.17)	$(1.71, 3.73) \times 10^{26}$	(3.53, 5.92)	$(0.85, 2.38) \times 10^{26}$
^{96}Zr			(1.01, 1.34)	$(7.90, 13.9) \times 10^{26}$	(1.43, 2.12)	$(3.16, 6.94) \times 10^{26}$
^{100}Mo			(2.22, 3.53)	$(1.46, 3.70) \times 10^{26}$	(2.91, 5.56)	$(0.59, 2.15) \times 10^{26}$
^{116}Cd			(1.83, 2.93)	$(1.95, 5.01) \times 10^{26}$	(2.30, 4.14)	$(0.98, 3.17) \times 10^{26}$
^{128}Te	2.26	1.10×10^{28}	(2.46, 3.77)	$(3.33, 7.81) \times 10^{27}$	(3.21, 5.65)	$(1.48, 4.59) \times 10^{27}$
^{130}Te	2.04	5.39×10^{26}	(2.27, 3.38)	$(1.65, 3.66) \times 10^{26}$	(2.92, 5.04)	$(7.42, 2.21) \times 10^{26}$
^{136}Xe	1.70	6.79×10^{26}	(1.17, 2.22)	$(3.59, 12.9) \times 10^{26}$	(1.57, 3.24)	$(1.68, 7.17) \times 10^{26}$